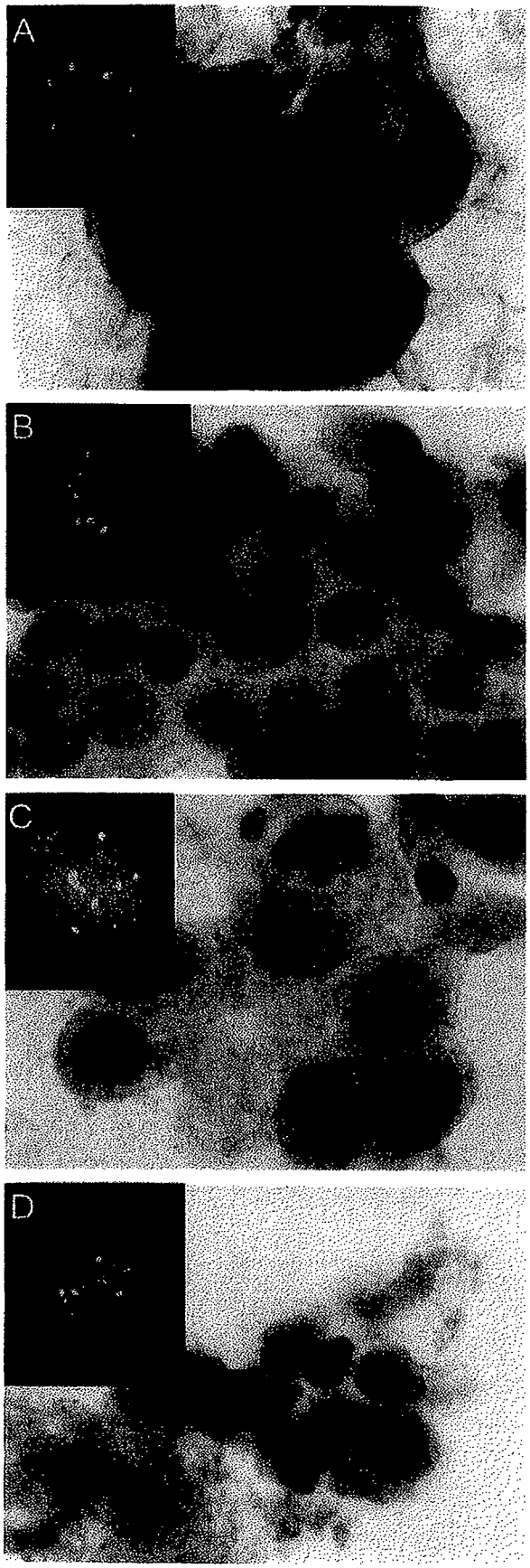

positive FISH findings. In these cases, the cytologic classifications were as follows: class II, five cases; and class IIIa, two cases. One case was cytology-positive and FISH-negative. In this case, the portion of aneusomic cells were observed to be 8 to 9%, which is just below the predetermined cutoff value.

Discussion

We demonstrated here the usefulness of FISH analyses in diagnosing lung cancer using various clinical specimens. Similar results about the effectiveness of FISH analyses have been reported by several authors. Schenk et al[20] examined 23 patients with lung cancer by FISH with probes specific for chromosomes 3, 8, 11, 12, 17, and 18 for malignant effusions and primary tumors. In that study, chromosomal alterations always consisted of gains in chromosomal signal numbers, and all chromosomes were found to be aneusomic to a similar extent. According to this observation, we used only two probes in the present study, which were specific for chromosomes 3 and 17.

Recently, Sokolova et al[21] analyzed BW specimens from 48 patients with lung cancer by FISH using four probes (*ie*, centromeric region of chromosome 1, 5p15, 8q24 (c-myc), and 7p12 [epidermal growth factor receptor]). In that report, FISH detected 15 of 18 specimens that were falsely negative by cytology. The sensitivity of FISH for the detection of lung cancer was 82% compared with 54% sensitivity by conventional cytology. The same group[22] used a similar FISH probe set to show that significantly higher frequencies of abnormal cells were found in each of the 20 surgical specimens of non-small cell carcinoma (100%) and in the 3 sputum specimens (100%) from lung cancer patients. These probes detected a 4.8 to 7.3% rate of abnormal copy numbers in normal control specimens. In these retrospective studies, FISH detected lung cancer cells in touch preparations of resected tumors and BWs. Thus, we planned a prospective study to compare conventional cytology with FISH using various specimens from lung lesions.

In our study, we determined the cutoff value for the percentage ofhyperdisomic cells to be 10%, be-

FIGURE 3. Hyperdisomic cells detected by FISH. Red signals are the centromeric region of chromosome 3, and green signals are the centromeric region of chromosome 17.Representative findings of conventional cytology (Papanicolaou stain, original ×400) and FISH in the same cases, as follows: *top left*, *A*: adenocarcinoma (case 39); *top right*, *B*: squamous cell carcinoma (case 1); *bottom left*, *C*: large cell carcinoma (case 24); and *bottom right*, *D*: small cell carcinoma (case 11).

cause we often count ≦6% hyperdisomic cells in normal cell specimens, probably due to counting sister chromatids as two copies. When we set the cutoff value at 10%, a specificity of 100% and a sensitivity of 87.1% were obtained by FISH, whereas the sensitivity of cytology was 71.8%. As a result, we successfully detected seven lung cancer cases that were cytology-negative. Among these cases, two were class IIIa that we could not diagnose as malignant based on morphologic features. FISH may provide decisive information for the detection of malignancies, especially cases with IIIa classification.

Although the sensitivity of FISH is superior to that of conventional cytology, there are some disadvantages to FISH analyses. First, we do not generate information about the histologic type of lung cancer since we cannot observe morphologic features. Second, FISH is expensive. Third, FISH signal counting under fluorescence microscopy is time-consuming. Thus, the present FISH assay system probably can play a complementary role to that of conventional cytology.

We had five cases that we could not correctly diagnose by FISH. There are two possible reasons for our false-negative FISH results. One would be the failure to obtain proper cell material from the lesion, resulting in the absence of cancer cells on the slide. The other would be that the cancer cells were near-diploid, such that we could not detect aneusomy in two target chromosomes. We could probably detect more aneusomic cells using additional suitable probes for other chromosomes or chromosomal regions as reported by Romeo et al,[22] who successfully diagnosed 100% of lung cancer cases by FISH using a set of four probes. In our previous study,[23] chromosomal instability detected by FISH was associated with poor survival in patients with lung cancer. The finding of multiple chromosomal changes by FISH may be used as a prognostic factor and in the selection of patients for different therapeutic programs in the future.

In conclusion, FISH can detect lung cancer cells with aneusomy in various clinical specimens. The sensitivity was superior to that of conventional cytology. FISH should be used in conjunction with conventional cytology.

REFERENCES

1 Muers M, Boddington M, Cole M, et al. Cytological sampling at fibreoptic bronchoscopy: comparison of catheter aspirates and brush biopsies. Thorax 1982; 37:457–461

2 Schenk D, Bryan C, Bower J, et al. Transbronchial needle aspiration in the diagnosis of bronchogenic carcinoma. Chest 1987; 92:83–85

3 Saji H, Nakamura H, Tsuchida T, et al. The incidence and the risk of pneumothorax and chest tube placement after percutaneous CT-guided lung biopsy: the angle of the needle trajectory is a novel predictor. Chest 2002; 121:1521–1526

4 Ng A, Horak G. Factors significant in the diagnostic accuracy of lung cytology in bronchial washing and sputum samples: I. Bronchial washings. Acta Cytol 1983; 27:391–396

5 Papanicolaou G. Criteria of malignancy. In: Atlas of exfoliative cytology. Cambridge, MA: Harvard University Press, 1954; 13–21

6 Choma D, Daures J-P, Quantin X, et al. Aneuploidy and prognosis of non-small-cell lung cancer: a meta-analysis of published data. Br J Cancer 2001; 85:14–22

7 Nowell P. The clonal evolution of tumor cell populations. Science 1976; 194:23–28

8 Hoglund M, Gisselsson D, Sall T, et al. Coping with complexity. Multivariate analysis of tumor karyotypes. Cancer Genet Cytogenet 2002; 135:103–109

9 Lengauer C, Kinzler K, Vogelstein B. Genetic instabilities in human cancers. Nature 1998; 396:643–649

10 Duesberg P, Rausch C, Rasnick D, et al. Genetic instability of cancer cells is proportional to their degree of aneuploidy. Proc Natl Acad Sci U S A 1998; 95:13692–13697

11 Cahill D, Lengauer C, Yu J, et al. Mutations of mitotic checkpoint genes in human cancers. Nature 1998; 392:300–303

12 Pihan G, Doxsey S. The mitotic machinery as a source of genetic instability in cancer. Semin Cancer Biol 1999; 9:289–302

13 Pinkel D, Straume T, Gray J. Cytogenetic analysis using quantitative, high-sensitivity, fluorescence hybridization. Proc Natl Acad Sci U S A 1986; 83:2934–2938

14 Gingrich J, Shadravan F, Lowry S. A fluorescence *in situ* hybridization map of human chromosome 21 consisting of 30 genetic and physical markers on the chromosome: localization of 137 additional YAC and cosmid clones with respect to this map. Genomics 1993; 17:98–105

15 Kuo W, Tenjin H, Segraves R, et al. Detection of aneuploidy involving chromosomes 13, 18, or 21, by fluorescence *in situ* hybridization (FISH) to interphase and metaphase amniocytes. Am J Hum Genet 1991; 49:112–119

16 Kallioniemi O, Kallioniemi A, Kurisu W, et al. ERBB2 amplification in breast cancer analyzed by fluorescence *in situ* hybridization. Proc Natl Acad Sci U S A 1992; 89:5321–5325

17 Gray J, Collins C, Henderson I, et al. Molecular cytogenetics of human breast cancer. Cold Spring Harb Symp Quant Biol 1994; 59:645–652

18 Hiraguri S, Godfrey T, Nakamura H, et al. Mechanisms of inactivation of E-cadherin in breast cancer cell lines. Cancer Res 1998; 58:1972–1977

19 Mountain C. Revisions in the International System for Staging Lung Cancer. Chest 1997; 111:1710–1717

20 Schenk T, Ackermann J, Brunner C, et al. Detection of chromosomal aneuploidy by interphase fluorescence *in situ* hybridization in bronchoscopically gained cells from lung cancer patients. Chest 1997; 111:1691–1696

21 Sokolova I, Bubendorf L, O'Hare A, et al. A fluorescence *in situ* hybridization-based assay for improved detection of lung cancer cells in bronchial washing specimens. Cancer 2002; 96:306–315

22 Romeo M, Sokolova I, Morrison L, et al. Chromosomal abnormalities in non-small cell lung carcinomas and in bronchial epithelia of high-risk smokers detected by multi-target interphase fluorescence *in situ* hybridization. J Mol Diagn 2003; 5:103–112

23 Nakamura H, Saji H, Idiris A, et al. Chromosomal instability detected by fluorescence *in situ* hybridization in surgical specimens of non-small cell lung cancer is associated with poor survival. Clin Cancer Res 2003; 9:2294–2299

Quantitative Detection of Lung Cancer Cells by Fluorescence In Situ Hybridization: Comparison With Conventional Cytology

Haruhiko Nakamura, Idiris Aute, Norihito Kawasaki, Masahiko Taguchi, Tatsuo Ohira and Harubumi Kato

Chest 2005;128;906-911
DOI 10.1378/chest.128.2.906

VOLUME 23 · NUMBER 6 · FEBRUARY 20 2005

JOURNAL OF CLINICAL ONCOLOGY

ORIGINAL REPORT

Randomized Pharmacokinetic and Pharmacodynamic Study of Docetaxel: Dosing Based on Body-Surface Area Compared With Individualized Dosing Based on Cytochrome P450 Activity Estimated Using a Urinary Metabolite of Exogenous Cortisol

Noboru Yamamoto, Tomohide Tamura, Haruyasu Murakami, Tatsu Shimoyama, Hiroshi Nokihara, Yutaka Ueda, Ikuo Sekine, Hideo Kunitoh, Yuichiro Ohe, Tetsuro Kodama, Mikiko Shimizu, Kazuto Nishio, Naoki Ishizuka, and Nagahiro Saijo

From the Division of Internal Medicine, National Cancer Center Hospital; Pharmacology Division and Cancer Information and Epidemiology Division, National Cancer Center Research Institute, Tokyo, Japan.

Submitted November 7, 2003; accepted August 19, 2004.

Supported in part by a Grant-in-Aid for Cancer Research (9-25) from the Ministry of Health, Labor, and Welfare, Tokyo, Japan.

Presented in part at the 38th Annual Meeting of the American Society of Clinical Oncology, May 18-21, 2002, Orlando, FL.

Authors' disclosures of potential conflicts of interest are found at the end of this article.

Address reprint requests to Tomohide Tamura, MD, Division of Internal Medicine, National Cancer Center Hospital, 5-1-1, Tsukiji, Chuo-ku, Tokyo, 104-0045, Japan; e-mail: ttamura@ncc.go.jp.

0732-183X/05/2306-1061/$20.00

DOI: 10.1200/JCO.2005.11.036

ABSTRACT

Purpose

Docetaxel is metabolized by cytochrome P450 (CYP3A4) enzyme, and the area under the concentration-time curve (AUC) is correlated with neutropenia. We developed a novel method for estimating the interpatient variability of CYP3A4 activity by the urinary metabolite of exogenous cortisol (6-beta-hydroxycortisol [6-β-OHF]). This study was designed to assess whether the application of our method to individualized dosing could decrease pharmacokinetic (PK) and pharmacodynamic (PD) variability compared with body-surface area (BSA)–based dosing.

Patients and Methods

Fifty-nine patients with advanced non–small-cell lung cancer were randomly assigned to either the BSA-based arm or individualized arm. In the BSA-based arm, 60 mg/m^2 of docetaxel was administered. In the individualized arm, individualized doses of docetaxel were calculated from the estimated clearance (estimated clearance = 31.177 + [7.655 × 10^{-4} × total 6-β-OHF] − [4.02 × alpha-1 acid glycoprotein] − [0.172 × AST] − [0.125 × age]) and the target AUC of 2.66 mg/L · h.

Results

In the individualized arm, individualized doses of docetaxel ranged from 37.4 to 76.4 mg/m^2 (mean, 58.1 mg/m^2). The mean AUC and standard deviation (SD) were 2.71 (range, 2.02 to 3.40 mg/L · h) and 0.40 mg/L · h in the BSA-based arm, and 2.64 (range, 2.15 to 3.07 mg/L · h) and 0.22 mg/L · h in the individualized arm, respectively. The SD of the AUC was significantly smaller in the individualized arm than in the BSA-based arm ($P < .01$). The percentage decrease in absolute neutrophil count (ANC) averaged 87.1% (range, 59.0 to 97.7%; SD, 8.7) in the BSA-based arm, and 87.4% (range, 78.0 to 97.2%; SD, 6.1) in the individualized arm, suggesting that the interpatient variability in percent decrease in ANC was slightly smaller in the individualized arm.

Conclusion

The individualized dosing method based on the total amount of urinary 6-β-OHF after cortisol administration can decrease PK variability of docetaxel.

J Clin Oncol 23:1061-1069. © 2005 by American Society of Clinical Oncology

INTRODUCTION

Many cytotoxic drugs have narrow therapeutic windows despite having a large interpatient pharmacokinetic (PK) variability. The doses of these cytotoxic drugs are usually calculated on the basis of body-surface area (BSA). Although several physiologic functions are proportional to BSA, systemic exposure to a drug is only partially related to

this parameter.[1-3] Consequently, a large interpatient PK variability is seen when doses are based on BSA. This large interpatient PK variability can result in undertreatment with inappropriate therapeutic effects in some patients, or in overtreatment with unacceptable severe toxicities in others. Understanding interpatient PK variability is important for optimizing anticancer treatments. Factors that affect PK variability include drug absorption, metabolism, and excretion. Among these factors, drug metabolism is regarded as a major factor causing PK variability. Unfortunately, however, no simple and practical method for estimating the interpatient variability of drug metabolism is available. If drug metabolism in each patient could be predicted, individualized dosing could be performed to optimize drug exposure while minimizing unacceptable toxicity.

Docetaxel is a cytotoxic agent that promotes microtubule assembly and inhibits depolymerization to free tubulin, resulting in the blockage of the M phase of the cell cycle.[4] Docetaxel has shown promising activity against several malignancies, including non–small-cell lung cancer, and is metabolized by hepatic CYP3A4 enzyme.[5-15]

Human CYP3A4 is a major cytochrome P450 enzyme that is present abundantly in human liver microsomes and is involved in the metabolism of a large number of drugs, including anticancer drugs.[16-18] This enzyme exhibits a remarkable interpatient variation in activity as high as 20-fold, which accounts for the large interpatient differences in the disposition of drugs that are metabolized by this enzyme.[19-22] Several noninvasive in vivo probes for estimating the interpatient variability of CYP3A4 activity have been reported and include the erythromycin breath test, the urinary dapsone recovery test, measurement of midazolam clearance (CL), and measurement of the ratio of endogenous urinary 6-beta-hydroxycortisol (6-β-OHF) to free-cortisol (FC).[23-27] The erythromycin breath test and the measurement of midazolam CL are the best validated, and both have been shown to predict docetaxel CL in patients.[28,29] However, neither probe has been used in a prospective study to validate the correlations observed, or to test their utility in guiding individualized dosing.

We developed a novel method for estimating the interpatient variability of CYP3A4 activity by urinary metabolite of exogenous cortisol. The total amount of 24-hour urinary 6-β-OHF after cortisol administration (total 6-β-OHF) is significantly correlated with docetaxel CL, which is metabolized by the CYP3A4 enzyme. We also illustrate the possibility that individualized dosing to optimize drug exposure and decrease interpatient PK variability could be performed using this method.[30]

We conducted a prospective, randomized PK and pharmacodynamic (PD) study of docetaxel comparing BSA-based dosing and individualized dosing based on the interpatient variability of CYP3A4 activity, as estimated by a urinary metabolite of exogenous cortisol. The objective of this study was to assess whether the application of our method to individualized dosing could decrease PK and PD variability of docetaxel compared with BSA-based dosing.

PATIENTS AND METHODS

Patient Selection

Patients with histologically or cytologically documented advanced or metastatic non–small-cell lung cancer were eligible for this study. Other eligibility criteria included the following: age $\geq$ 20 years; Eastern Cooperative Oncology Group performance status of 0, 1, or 2; 4 weeks of rest since any previous anticancer therapy; and adequate bone marrow (absolute neutrophil count [ANC] $\geq$ 2,000/μL and platelet count $\geq$ 100,000/μL), renal (serum creatinine level $\leq$ 1.5 mg/dL), and hepatic (serum total bilirubin level $\leq$ 1.5 mg/dL, AST level $\leq$ 150 U/L, and ALT level $\leq$ 150 U/L) function. Written informed consent was obtained from all patients before enrollment onto the study.

The exclusion criteria included the following: pregnancy or lactation; concomitant radiotherapy for primary or metastatic sites; concomitant chemotherapy with any other anticancer agents; treatment with steroids or any other drugs known to induce or inhibit CYP3A4 enzyme[17]; serious pre-existing medical conditions, such as uncontrolled infections, severe heart disease, diabetes, or pleural or pericardial effusions requiring drainage; and a known history of hypersensitivity to polysorbate 80. This study was approved by the institutional review board of the National Cancer Center.

Pretreatment and Follow-Up Evaluation

On enrollment onto the study, a history and physical examination were performed, and a complete differential blood cell count (including WBC count, ANC, hemoglobin, and platelets), and a clinical chemistry analysis (including serum total protein, albumin [ALB], bilirubin, creatinine, AST, ALT, gamma-glutamyltransferase, alkaline phosphatase [ALP], and alpha-1 acid glycoprotein [AAG]) were performed. Blood cell counts and a chemistry analysis except for AAG were performed at least twice a week throughout the study. Tumor measurements were performed every two cycles, and antitumor response was assessed by WHO standard response criteria. Toxicity was evaluated according to the National Cancer Institute Common Toxicity Criteria (version 2.0).

Study Design

This study was designed to assess whether the application of our method to individualized dosing could decrease PK and PD variability compared with BSA-based dosing. The primary end point was PK variability and the secondary end point was PD variability (ie, toxicity). In our previous study involving 29 patients who received 60 mg/m^2 of docetaxel, the area under the concentration-time curve (AUC) was calculated to be 2.66 $\pm$ 0.91 (mean $\pm$ standard deviation [SD]) mg/L $\cdot$ h.[30] We assumed that the variability of AUC, represented by the SD, could be reduced by 50% in the individualized arm compared with that in the BSA-based arm, and that AUC would be normally distributed. The required sample size was 25 patients per arm to detect this difference with a two-sided F test at α = .05 and a power of 0.914.

Patients were randomly assigned to either the BSA-based arm or individualized arm (Fig 1). In the BSA-based arm, each patient received a dose of 60 mg/m^2 of docetaxel. In the individualized arm, individualized doses of docetaxel were calculated from the estimated docetaxel CL after cortisol administration and the target AUC (described in the Docetaxel Administration section).

Cortisol Administration and Urine Collection

In the individualized arm, 300 mg of hydrocortisone (Banyu Pharmaceuticals Co, Tokyo, Japan) was diluted in 100 mL of 0.9%

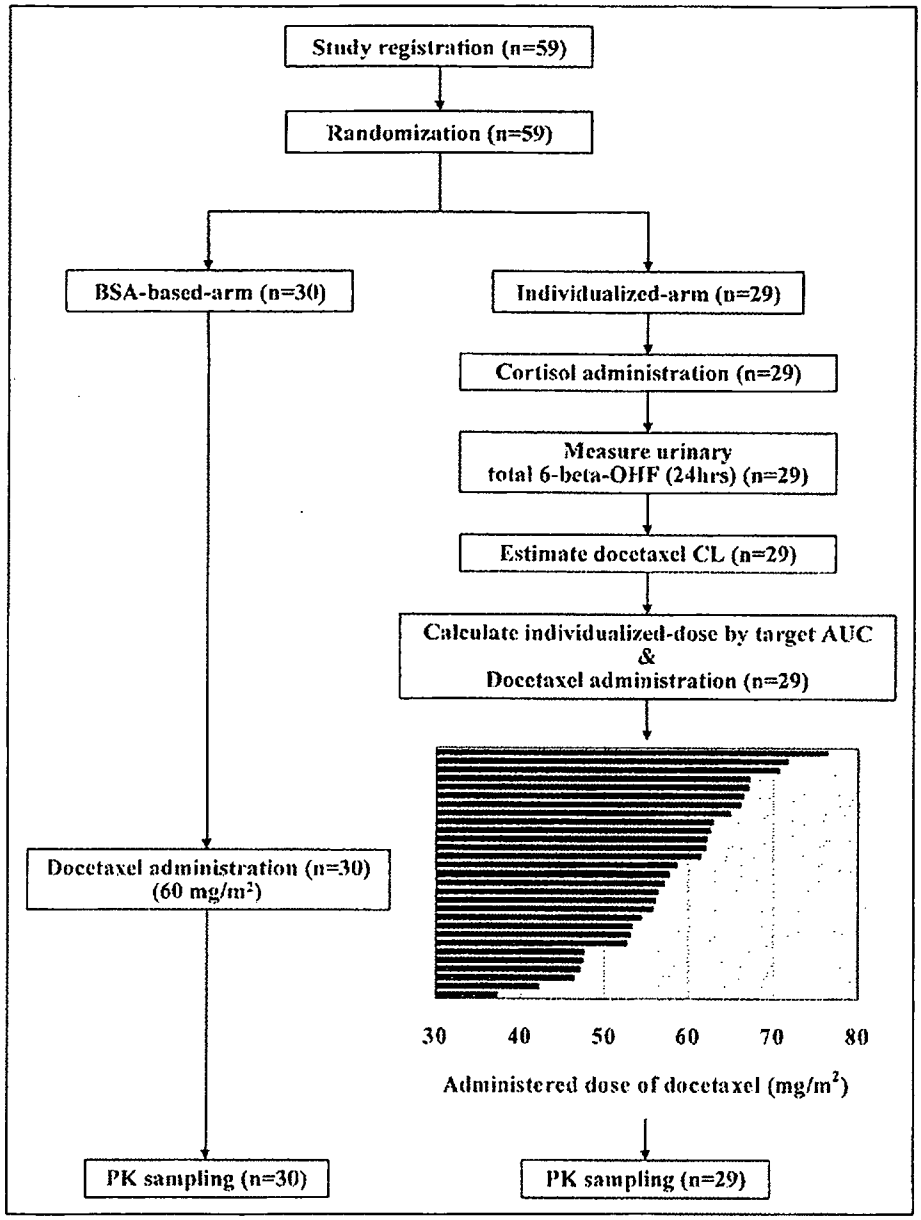

Fig 1. Study flow diagram and administered dose of docetaxel. PK, pharmacokinetic; AUC, area under the concentration-time curve; CL, clearance; 6-β-OHF, 6-beta-hydroxycortisol.

saline and administered intravenously for 30 minutes at 9 AM on day 1 in all patients to estimate the interpatient variability of CYP3A4 activity. After cortisol administration, the urine was collected for 24 hours. The total volume of the 24-hour collection was recorded, and a 5-mL aliquot was analyzed immediately.

Docetaxel Administration

Docetaxel (Taxotere; Aventis Pharm Ltd, Tokyo, Japan) was obtained commercially as a concentrated sterile solution containing 80 mg of the drug in 2 mL of polysorbate 80. In the BSA-based arm, a dose of 60 mg/m^2 of docetaxel was diluted in 250 mL of 5% glucose or 0.9% saline and administered by 1-hour intravenous infusion at 9 AM to all patients.

In the individualized arm, individualized dose of docetaxel was calculated from the estimated CL and the target AUC of 2.66 mg/L · h using the following equations:

$$\text{Estimated CL (L/h/m}^2) = 31.177 + (7.655 \times 10^{-4} \times \text{total-6-}\beta\text{-OHF [}\mu\text{g/d]}) - (4.02 \times \text{AAG [g/L]}) - (0.172 \times \text{AST [U/L]}) - (0.125 \times \text{age [years]})^{30}$$

$$\text{Individualized dose of docetaxel (mg/m}^2) = \text{estimated docetaxel CL (L/h/m}^2) \times \text{target AUC (2.66 mg/L} \cdot \text{h)}$$

At least 2 days after cortisol administration, individualized doses of docetaxel were diluted in 250 mL of 5% glucose or 0.9% saline and administered by 1-hour intravenous infusion at 9 AM to each patient. The doses of docetaxel in subsequent cycles of treatment were unchanged, and no prophylactic premedication to protect against docetaxel-related hypersensitivity reactions was administered in either of the treatment arms.

PK Study

Blood samples for PK studies were obtained from all of the patients during the initial treatment cycle. An indwelling cannula was inserted in the arm opposite that used for the drug infusion, and blood samples were collected into heparinized tubes. Blood samples were collected before the infusion; 30 minutes after the start of the infusion; at the end of the infusion; and 15, 30, and 60 minutes and 3, 5, 9, and 24 hours after the end of the infusion. All blood samples were centrifuged immediately at 4,000 rpm for 10 minutes, after which the plasma was removed and the samples were placed in polypropylene tubes, labeled, and stored at −20°C or colder until analysis.

PK parameters were estimated by the nonlinear least squares regression analysis method (WinNonlin, Version 1.5; Bellkey Science Inc, Chiba, Japan) with a weighting factor of 1 per year.[2] Individual plasma concentration-time data were fitted to two- and three-compartment PK models using a zero-order infusion input and first-order elimination. The model was chosen on the basis of Akaike's information criteria.[31] The peak plasma concentration (C_{max}) was generated directly from the experimental data. AUC was extrapolated to infinity and determined based on the best-fitted curve; this measurement was then used to calculate the absolute CL (L/h), defined as the ratio of the delivered dosage (in milligrams) and AUC.

To assess PD effect of docetaxel, the percentage decrease in ANC was calculated according to the following formula: % decrease in ANC = (pretreatment ANC − nadir ANC)/(pretreatment ANC) × 100.

Measurements

The concentration of urinary 6-β-OHF was measured by reversed phase high-performance liquid chromatography with UV absorbance detection according to previously published methods.[30,32,33]

Docetaxel concentrations in plasma were also measured by solid-phase extraction and reversed phase high-performance liquid chromatography with UV detection according to the previously published method.[30,34] The detection limit corresponded to a concentration of 10 ng/mL.

Statistical Analysis

Fisher's exact test or χ^2 test was used to compare categoric data, and Student's t test was used for continuous variables. The strength of the relationship between the estimated docetaxel CL and the observed docetaxel CL was assessed by least squares linear regression analysis. The interpatient variability of AUC for each arm was evaluated by determining the SD and was compared by F test. Biases, or the mean AUC value in each arm minus the target AUC (2.66 mg/L · h), were also compared between the arms by Student's t test.

A two-sided P value of ≤ .05 or less was considered to indicate statistical significance. All statistical analyses were performed using SAS software version 8.02 (SAS Institute, Cary, NC).

RESULTS

Patient Characteristics

Between October 1999 and May 2001, 59 patients were enrolled onto the study and randomly assigned to either the BSA-based arm (n = 30) or the individualized arm (n = 29). All 59 patients were assessable for PK and PD analyses. The pretreatment characteristics of the 59 patients are listed in Table 1. The baseline characteristics were well balanced between the arms except for three laboratory parameters: ALB, AAG, and ALP. These three parameters were not included in the eligibility criteria. The majority of patients (95%) had a performance status of 0 or 1. Twenty (67%) and 16 (55%) patients had been treated with platinum-based chemotherapy in the BSA-based arm and individualized arm, respectively. Only two patients in the individualized arm had liver metastasis, and most of the patients had good hepatic functions.

Individualized Dosing of Docetaxel

In the individualized arm, the total amount of 24-hour urinary 6-β-OHF after cortisol administration (total 6-β-OHF) was 9,179.6 ± 3,057.7 μg/d (mean ± SD), which was similar to the result of our previous study.[30] The estimated docetaxel CL was 21.9 ± 3.5 L/h/m^2 (mean ± SD), and individualized dose of docetaxel ranged from 37.4 to 76.4 mg/m^2 (mean, 58.1 mg/m^2; Fig 1).

PK

Docetaxel PK data were obtained from all 59 patients during the first cycle of therapy, and PK parameters are listed in Table 2. Drug levels declined rapidly after infusion and could be determined to a maximum of 25 hours. The concentration of docetaxel in plasma was fitted to a biexponential equation, which was consistent with previous reports.[30,35-38] The mean alpha and beta half-lives were 9.2 minutes and 5.0 hours in the BSA-based arm and 9.2 minutes and 7.4 hours in the individualized arm, respectively.

In the BSA-based arm, docetaxel CL was 22.6 ± 3.4 L/h/m^2 (mean ± SD), and AUC averaged 2.71 mg/L · h (range, 2.02 to 3.40 mg/L · h). In the individualized arm, docetaxel CL was 22.1 ± 3.4 L/h/m^2, and AUC averaged 2.64 mg/L · h (range, 2.15 to 3.07 mg/L · h). The least squares linear regression analysis showed that the observed docetaxel CL was well estimated in the individualized arm (r^2 = 0.821; Fig 2).

The SDs of AUC in the BSA-based arm and in the individualized arm were 0.40 and 0.22, respectively, and the ratio of SD in the individualized arm to that in the BSA-based arm was 0.538 (95% CI, 0.369 to 0.782). The biases from the target AUC in the BSA-based arm and in the individualized arm were 0.047 (95% CI, −0.104 to 0.198) and −0.019 (95% CI, −0.102 to 0.064), respectively, with no significant difference. The interpatient variability of

Table 1. Patient Characteristics

Characteristic	BSA-Based Arm No. of Patients	%	Individualized Arm No. of Patients	%	P
Enrolled	30		29		
Eligible	30	100	29	100	
Age, years					.62
Median	61		62		
Range	52-73		45-73		
Sex					
Male	25	83	19	66	.14
Female	5	17	10	34	
ECOG PS					
0	7	23	1	3	.08
1	22	73	26	90	
2	1	3	2	7	
Prior treatment					
None	4	13	4	14	.99
Surgery	11	37	9	31	.65
Radiotherapy	13	43	10	34	.49
Chemotherapy	21	70	18	62	.52
Platinum-based regimens	20	67	16	55	.37
Site of disease					
Lung	23	77	28	97	.10
Liver	0	0	2	7	.24
Pleura	8	27	12	41	.23
Bone	7	23	9	31	.71
Extrathoracic lymph nodes	0	33	10	34	.93
Laboratory parameters					
ALB, g/L					.02
Median	38		35		
Range	26-45		24-44		
AAG, g/L					.04
Median	1.00		1.25		
Range	0.28-2.15		0.64-2.54		
AST, U/L					.67
Median	21		22		
Range	10-40		7-41		
ALT, U/L					.88
Median	18		18		
Range	6-54		4-45		
ALP, U/L					.03
Median	249		324		
Range	129-540		185-986		

Abbreviations: ECOG, Eastern Cooperative Oncology Group; PS, performance status, ALB, serum albumin; AAG, alpha-1-acid glycoprotein; ALP, serum alkaline phosphatase.

AUC was significantly smaller in the individualized arm than in the BSA-based arm ($P < .01$; Fig 3).

PD

In both arms, neutropenia was the predominant toxicity related to docetaxel treatment, and 28 of 30 (93%) patients in the BSA-based arm and 25 of 29 (86%) patients in the individualized arm had grade 3 or 4 neutropenia.

Table 2. Docetaxel PK Parameters

Parameters	BSA-Based Arm (n = 30)	Individualized Arm (n = 29)
C_{max}, μg/mL	0.36-2.70	0.99-2.41
$t_{1/2}$ alpha*, minutes	9.2 ± 3.3	9.2 ± 2.7
$t_{1/2}$ beta*, hours	5.0 ± 4.8	7.4 ± 11.7
CL* L/h	37.6 ± 6.3	34.8 ± 7.1
CL* L/h/m²	22.6 ± 3.4	22.1 ± 3.4
AUC		
Mean mg/L · h	2.71	2.64
Range mg/L · h	2.02-3.40	2.15-3.07
Median	2.65	2.66
SD	0.40	0.22

Abbreviations: PK, pharmacokinetic; BSA, body-surface area; CL, clearance; AUC, area under concentration-time curve; SD, standard deviation.
*Data represent mean ± SD.

Nonhematologic toxicities, such as gastrointestinal and hepatic toxicities (ie, hyperbilirubinemia, aminotransferase elevations), were mild in both arms.

PD effects shown as the percentage decrease in ANC are listed in Table 3. The percentage decrease in ANC for the BSA-based arm and individualized arm were 87.1% (range, 59.0 to 97.7%; SD, 8.7) and 87.5% (range, 78.0 to 97.2%; SD, 6.1), respectively, suggesting that the interpatient variability in the percentage decrease in ANC was slightly smaller in the individualized arm than in the BSA-based arm (Fig 4). The response rates between the two arms were similar; five of 30 (16.7%) and four of 29 (13.8%) patients

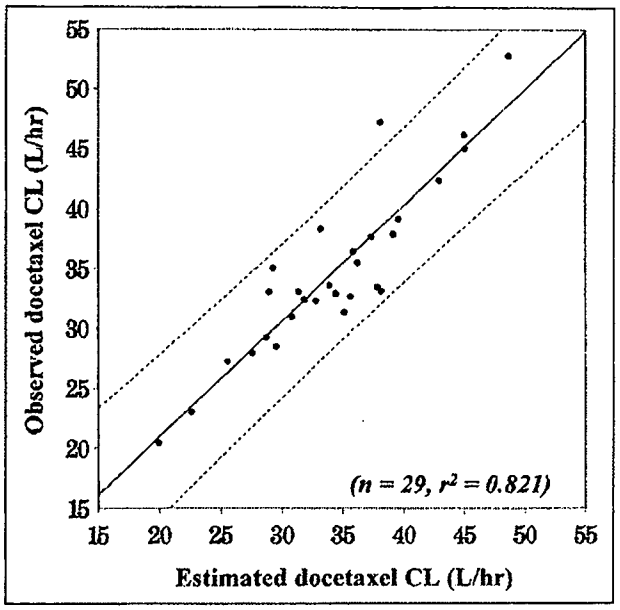

Fig 2. Correlation between the estimated and observed docetaxel clearance (CL) in the individualized arm (n = 29). (—) Linear regression line ($r^2 = 0.821$); (– – –) 95% CIs for individual estimates.

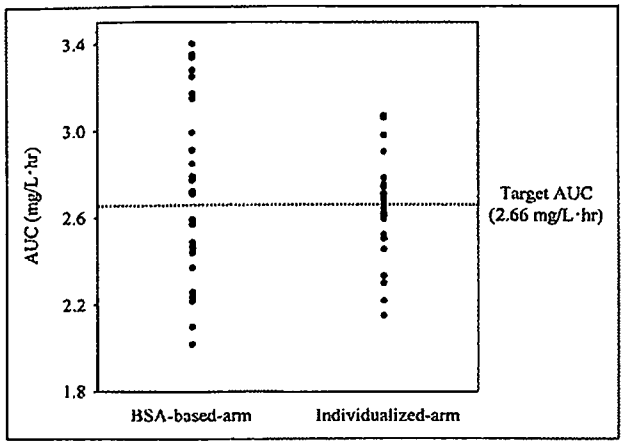

Fig 3. Comparison of area under the concentration-time curve (AUC) variability between the arms ($P < .01$; F test). BSA, body-surface area.

achieved a partial response in the BSA-based arm and individualized arm, respectively.

DISCUSSION

In oncology practice, the prescribed dose of most anticancer drugs is currently calculated from BSA of individual patients to reduce the interpatient variability of drug exposure. However, PK parameters, such as CL of many anticancer drugs, are not related to BSA.[2,39-43] Although PK parameters of docetaxel are correlated with BSA, individualized dosing based on individual metabolic capacities could further decrease the interpatient variability.[43]

CYP3A4 plays an important role in the metabolism of many drugs, including anticancer agents such as docetaxel, paclitaxel, vinorelbine, and gefitinib. This enzyme exhibits a large interpatient variability in metabolic activity, accounting for the large interpatient PK and PD variability. We have developed a novel method of estimating the interpatient variability of CYP3A4 activity by urinary metabolite of exogenous cortisol. That is, the total amount of 24-hour urinary 6-β-OHF after cortisol administration was highly correlated with docetaxel CL. We conducted a prospective randomized PK and PD study of docetaxel to evaluate whether the application of our method to individualized dosing could decrease PK and PD variability compared with BSA-based dosing.

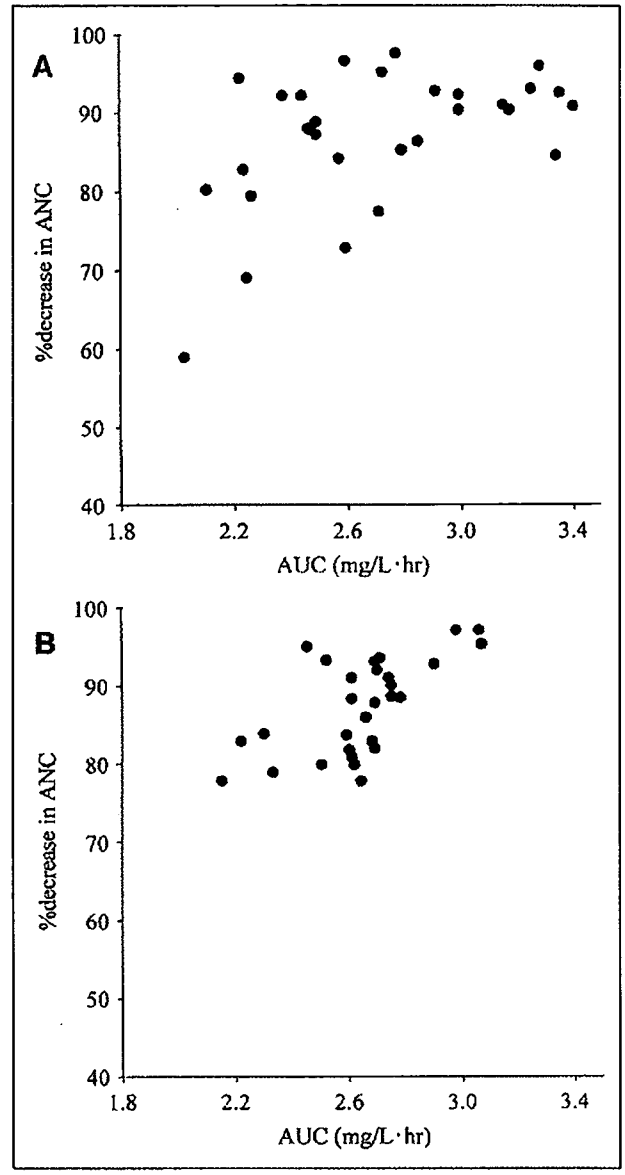

Fig 4. Correlation between area under the concentration-time curve (AUC) and percentage decrease in absolute neutrophil count (ANC) in each arm. (A) body-surface area–based arm; (B) individualized arm.

Table 3. Percentage Decrease in ANC

Parameters	BSA-Based Arm (n = 30)	Individualized Arm (n = 29)
Percentage decrease in ANC, %		
Mean	87.1	87.4
Range	59.0-97.7	78.0-97.2
Median	89.7	88.4
SD	8.7	8.1

Abbreviations: ANC, absolute neutrophil count; BSA, body-surface area; SD, standard deviation.

The study by Hirth et al[28] showed a good correlation between the result of the erythromycin breath test and docetaxel CL, and the study by Goh et al[29] showed a good correlation between the midazolam CL and docetaxel CL. In our study, we prospectively validated the correlation between docetaxel CL and our previously published method using the total amount of urinary 6-β-OHF after

cortisol administration in the individualized arm. As shown in Fig 2, the observed docetaxel CL was well estimated, and the equation for the estimation of docetaxel CL developed in our previous study was found to be reliable and reproducible. The target AUC in the individualized arm was set at 2.66 mg/L · h. This value was the mean value from our previous study, in which 29 patients were treated with 60 mg/m^2 of docetaxel. Individualized doses of docetaxel ranged from 37.4 to 76.4 mg/m^2 and were lower than expected.

The SD of AUC in the individualized arm was about 46.2% smaller than that in the BSA-based arm, a significant difference; this result seems to indicate that the application of our method to individualized dosing can reduce the interpatient PK variability. Assuming that the variability of AUC could be decreased 46.2% by individualized dosing applying our method, overtreatment could be avoided in 14.5% of BSA-dosed patients by using individualized dosing (Fig 5, area A), and undertreatment could be avoided in another 14.5% of these patients (Fig 5, area B). We considered that neutropenia could be decreased with patients in area A by individualized dosing. However, it is unknown whether the therapeutic effect of docetaxel could be improved in the patients in area B by individualized dosing because no significant positive correlation has been found between docetaxel AUC and antitumor response in patients with non–small-cell lung cancer.[43] In this study, seven of 30 (23.3%) and two of 30 (6.7%) patients in the BSA-based arm were included in area A and B, respectively (Figs 3 and 5).

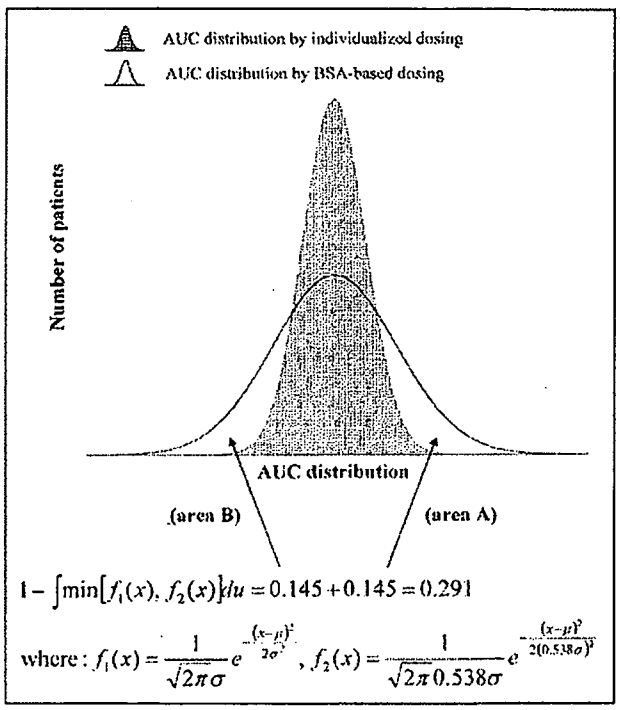

Fig 5. Simulated comparison of area under the concentration-time curve (AUC) distribution between body-surface area (BSA) –based dosing and individualized dosing when the variability of AUC is decreased 46.2% by individualized dosing applied using our method.

As shown in Figure 4, the percentage decrease in ANC was well correlated with AUC in both arms, which was similar to previous reports.[37,43] It was also indicated that the interpatient variability in the percentage decrease in ANC was slightly smaller in the individualized arm than in the BSA-based arm; however, this difference was not significant. The response rates between the two arms were similar. Although the interpatient PK variability could be decreased by individualized dosing in accordance with our method, the interpatient PD variability such as toxicity and the antitumor response could not be decreased. Several reasons could be considered.

With regard to toxicity, the pretreatment characteristics of the patients in this study were highly variable. More than half of the patients in each arm had previously received platinum-based chemotherapy, and more than 30% had received radiotherapy. The laboratory parameters (ie, ALB, AAG, and ALP) were not balanced across the arms, although they were not included in the eligibility criteria (Table 1). These variable pretreatment characteristics and unbalanced laboratory parameters may have influenced the frequency and severity of the hematologic toxicity as well as the pharmacokinetic profiles. The antitumor effect may have been influenced by the intrinsic sensitivity of tumors, the variable pretreatment characteristics, and the imbalance in laboratory parameters. Non–small-cell lung cancer is a chemotherapy-resistant tumor. The response rate for docetaxel ranges from 18% to 38%,[5] and no significant positive correlation between docetaxel AUC and antitumor response has been found. We considered it quite difficult to control the interpatient PD variability by controlling the interpatient PK variability alone. Although we did not observe any outliers in either arm, such as the two outliers with severe toxicity observed in the study by Hirth et al,[28] our method may be more useful for identifying such outliers. If we had not excluded patients with more abnormal liver function or a history of liver disease by the strict eligibility criteria, the results with the two dosing regimens may have been more different, and the interpatient PD variability, such as the percentage decrease in ANC, may have been smaller in the individualized arm than in the BSA-based arm. Furthermore, the primary end point of this study was PK variability, evaluated by the SD of AUC in both arms, and the sample size was significantly underpowered to evaluate whether the application of our method to individualized dosing could decrease PD variability compared with BSA-based dosing.

For the genotypes of CYP3A4, several genetic polymorphisms have been reported (http://www.imm.ki.se/CYPalleles/); however, a clear relationship between genetic polymorphisms and the enzyme activity of CYP3A4 has not been reported. Our phenotype-based

individualized dosing using the total amount of urinary 6-β-OHF after cortisol administration produced good results. However, this method is somewhat complicated, and a simpler method would be of great use. We analyzed the expression of CYP3A4 mRNA in the peripheral-blood mononuclear cells of the 29 patients in the individualized arm. No correlation was observed between the expression level of CYP3A4 mRNA and docetaxel CL or the total amount of urinary 6-β-OHF after cortisol administration (data not shown).

In conclusion, the individualized dosing of docetaxel using the total amount of urinary 6-β-OHF after cortisol administration is useful for decreasing the interpatient PK variability compared with the conventional BSA-based method of dosing. This method may be useful for individualized chemotherapy.

Authors' Disclosures of Potential Conflicts of Interest

The authors indicated no potential conflicts of interest.

References

1. Sawyer M, Ratain MJ: Body surface area as a determinant of pharmacokinetics and drug dosing. Invest New Drugs 19:171-177, 2001
2. Gurney H: Dose calculation of anticancer drugs: A review of the current practice and introduction of an alternative. J Clin Oncol 14: 2590-2611, 1996
3. Ratain MJ: Body-surface area as a basis for dosing of anticancer agents: Science, myth, or habit? J Clin Oncol 16:2297-2298, 1998
4. Ringel I, Horwitz SB: Studies with RP 56976 (Taxotere): A semisynthetic analogue of taxol. J Natl Cancer Inst 83:288-291, 1991
5. Cortes JE, Pazdur R: Docetaxel. J Clin Oncol 13:2643-2655, 1995
6. Fossella FV, Lee JS, Murphy WK, et al: Phase II study of docetaxel for recurrent or metastatic non-small-cell lung cancer. J Clin Oncol 12:1238-1244, 1994
7. Fossella FV, Lee JS, Shin DM, et al: Phase II study of docetaxel for advanced or metastatic platinum-refractory non-small-cell lung cancer. J Clin Oncol 13:645-651, 1995
8. Gandara DR, Vokes E, Green M, et al: Activity of docetaxel in platinum-treated non-small-cell lung cancer: Results of a phase II multicenter trial. J Clin Oncol 18:131-135, 2000
9. Kunitoh H, Watanabe K, Onoshi T, et al: Phase II trial of docetaxel in previously untreated advanced non-small-cell lung cancer: A Japanese cooperative study. J Clin Oncol 14:1649-1655, 1996
10. Fossella FV, DeVore R, Kerr RN, et al: Randomized phase III trial of docetaxel versus vinorelbine or ifosfamide in patients with advanced non-small-cell lung cancer previously treated with platinum-containing chemotherapy regimens: The TAX 320 Non-Small Cell Lung Cancer Study Group. J Clin Oncol 18:2354-2362, 2000
11. Shepherd FA, Dancey J, Ramlau R, et al: Prospective randomized trial of docetaxel versus best supportive care in patients with non–small-cell lung cancer previously treated with platinum-based chemotherapy. J Clin Oncol 18:2095-2103, 2000
12. Hudis CA, Seidman AD, Crown JP, et al: Phase II and pharmacologic study of docetaxel as initial chemotherapy for metastatic breast cancer. J Clin Oncol 14:58-65, 1996
13. Trudeau ME, Eisenhauer EA, Higgins BP, et al: Docetaxel in patients with metastatic breast cancer: A phase II study of the National Cancer Institute of Canada-Clinical Trials Group. J Clin Oncol 14:422-428, 1996
14. Chan S, Friedrichs K, Noel D, et al: Prospective randomized trial of docetaxel versus doxorubicin in patients with metastatic breast cancer: The 303 Study Group. J Clin Oncol 17:2341-2354, 1999
15. Marre F, Sanderink GJ, de Sousa G, et al: Hepatic biotransformation of docetaxel (Taxotere) *in vitro*: Involvement of the CYP3A subfamily in humans. Cancer Res 56:1296-1302, 1996
16. Nelson DR, Koymans L, Kamataki T, et al: P450 superfamily: Update on new sequences, gene mapping, accession numbers and nomenclature. Pharmacogenetics 6:1-42, 1996
17. Lin JH, Lu AYH: Inhibition and induction of cytochrome P450 and the clinical implications. Clin Pharmacokinet 35:361-390, 1998
18. Parkinson A: An overview of current cytochrome P450 technology for assessing the safety and efficacy of new materials. Toxicol Pathol 24:45-57, 1996
19. Shimada T, Yamazaki H, Mimura M, et al: Interindividual variations in human liver cytochrome P-450 enzymes involved in the oxidation of drugs, carcinogens and toxic chemicals: Studies with liver microsomes of 30 Japanese and 30 Caucasians. J Pharmacol Exp Ther 270:414-423, 1994
20. Guengerich FP: Characterization of human microsomal cytochrome P450 enzymes. Annu Rev Pharmacol Toxicol 29:241-264, 1989
21. Guengerich FP, Turvy CG: Comparison of levels of human microsomal cytochrome P450 enzymes and epoxide hydrolase in normal and disease status using immunochemical analysis of surgical samples. J Pharmacol Exp Ther 256: 1189-1194, 1991
22. Hunt CM, Westerkam WR, Stave GM: Effects of age and gender on the activity of human hepatic CYP3A. Biochem Pharmacol 44: 275-283, 1992
23. Watkins PB, Turgeon DK, Saenger P, et al: Comparison of urinary 6-beta-cortisol and the erythromycin breath test as measures of hepatic P450IIIA (CYP3A) activity. Clin Pharmacol Ther 52:265-273, 1992
24. Kinirons MT, O'Shea D, Downing TE, et al: Absence of correlations among three putative *in vivo* probes of human cytochrome P4503A activity in young healthy men. Clin Pharmacol Ther 54:621-629, 1993
25. Hunt CM, Watkins PB, Saenger P, et al: Heterogeneity of CYP3A isoforms metabolizing erythromycin and cortisol. Clin Pharmacol Ther 51:18-23, 1992
26. Thummel KE, Shen DD, Podoll TD, et al: Use of midazolam as a human cytochrome P450 3A probe: II. Characterization of inter- and intra-individual hepatic CYP3A variability after liver transplantation. J Pharmacol Exp Ther 271:557-566, 1994
27. Thummel KE, Shen DD, Podoll TD, et al: Use of midazolam as a human cytochrome P450 3A probe: I. In vitro-in vivo correlations in liver transplant patients. J Pharmacol Exp Ther 271: 549-556, 1994
28. Hirth J, Watkins PB, Strawderman M, et al: The effect of an individual's cytochrome CYP3A4 activity on docetaxel clearance. Clin Cancer Res 6:1255-1258, 2000
29. Goh BC, Lee SC, Wang LZ, et al: Explaining interindividual variability of docetaxel pharmacokinetics and pharmacodynamics in Asians through phenotyping and genotyping strategies. J Clin Oncol 20:3683-3690, 2002
30. Yamamoto N, Tamura T, Kamiya Y, et al: Correlation between docetaxel clearance and estimated cytochrome P450 activity by urinary metabolite of exogenous cortisol. J Clin Oncol 18:2301-2308, 2000
31. Yamaoka K, Nakagawa T, Uno T: Application of Akaike's information criterion (AIC) in the evaluation of linear pharmacokinetic equations. J Pharmacokinet Biopharm 6:165-175, 1978
32. Nakamura J, Yakata M: Determination of urinary cortisol and 6 beta-hydroxycortisol by high performance liquid chromatography. Clin Chim Acta 149:215-224, 1985
33. Lykkesfeldt J, Loft S, Poulsen HE: Simultaneous determination of urinary free cortisol and 6 beta-hydroxycortisol by high-performance liquid chromatography to measure human CYP3A activity. J Chromatogr B Biomed Appl 660:23-29, 1994
34. Vergniol JC, Bruno R, Montay G, et al: Determination of Taxotere in human plasma by a semi-automated high-performance liquid chromatographic method. J Chromatogr 582:273-278, 1992
35. Taguchi T, Furue H, Niitani H, et al: Phase I clinical trial of RP 56976 (docetaxel) a new anticancer drug. Gan To Kagaku Ryoho 21:1997-2005, 1994
36. Burris H, Irvin R, Kuhn J, et al: Phase I clinical trial of Taxotere administered as either a 2-hour or 6-hour intravenous infusion. J Clin Oncol 11:950-958, 1993
37. Extra JM, Rousseau F, Bruno R, et al: Phase I and pharmacokinetic study of Taxotere (RP 56976; NSC 628503) given as a short

intravenous infusion. Cancer Res 53:1037-1042, 1993

38. Pazdur R, Newman RA, Newman BM, et al: Phase I trial of Taxotere: Five-day schedule. J Natl Cancer Inst 84:1781-1788, 1992

39. Mathijssen RHJ, Verweij J, de Jonge MJ, et al: Impact of body-size measures on irinotecan clearance: Alternative dosing recommendations. J Clin Oncol 20:81-87, 2002

40. De Jongh FE, Verweij J, Loos WJ, et al: Body-surface area-based dosing does not increase accuracy of predicting cisplatin exposure. J Clin Oncol 19:3733-3739, 2001

41. Gurney HP, Ackland S, Gebski V, et al: Factors affecting epirubicin pharmacokinetics and toxicity: Evidence against using body-surface area for dose calculation. J Clin Oncol 16:2299-2304, 1998

42. Loos WJ, Gelderblom H, Sparreboom A, et al: Inter- and intrapatient variability in oral topotecan pharmacokinetics: Implications for body-surface area dosage regimens. Clin Cancer Res 6:2685-2689, 2000

43. Bruno R, Hille D, Riva A, et al: Population pharmacokinetics/pharmacodynamics of docetaxel in phase II studies in patients with cancer. J Clin Oncol 16:187-196, 1998

Risk of Pleural Recurrence After Needle Biopsy in Patients With Resected Early Stage Lung Cancer

Haruhisa Matsuguma, MD, Rie Nakahara, MD, Tetsuro Kondo, MD, Yukari Kamiyama, MD, Kiyoshi Mori, MD, and Kohei Yokoi, MD

Divisions of Thoracic Surgery and Thoracic Diseases, Tochigi Cancer Center, Utsunomiya, Tochigi, Japan

Background. Concerning the complications resulting from percutaneous needle biopsy (PNB), although cases of tumor seeding into the needle track have occasionally been reported, there were only two cases of pleural recurrences to date. The aim of this study was to elucidate the real risk of pleural recurrence after needle biopsy in patients with resected early stage lung cancer.

Methods. Between 1986 and 2000, 335 patients with stage I nonsmall cell lung cancer underwent complete resection of the lung tumor. We retrospectively reviewed their medical records and investigated the relationship between the diagnostic methods used and the cancer recurrence patterns.

Results. Preoperative diagnoses were obtained for 290 patients; 220 were diagnosed by bronchoscopy and 66 by PNB. Among the patients without a preoperative diagnosis, 27 were diagnosed by intraoperative needle biopsy and 14 by wedge resection of the lung. Tumors diagnosed by needle biopsy including PNB and intraoperative needle biopsy were smaller and showed less vessel invasion than those diagnosed by other methods ($p < 0.01$). After surgical resection, 9 patients had pleural recurrence and 1 patient, needle track implantation. Seven of these 10 patients were diagnosed by needle biopsy using 18G cutting type needle. Pleural recurrence or needle track implantation was observed for 8.6% of the patients who underwent a needle biopsy, whereas it was 0.9% for patients who were examined using other diagnostic modalities ($p = 0.0009$).

Conclusions. Needle biopsy especially using a cutting-type biopsy needle can cause a pleural recurrence in addition to needle track implantation.

(Ann Thorac Surg 2005;80:2026–31)

Percutaneous needle biopsies (PNB) are widely used for the histologic diagnosis of a peripheral indeterminate pulmonary nodule. The overall sensitivity and specificity for diagnosing peripheral lung cancers were 90% and 97% respectively by meta-analysis [1], and even for tumors less than 2 cm in diameter the sensitivity was also as high as 91%.

Although fine-needle aspiration (FNA) is widely used method for performing PNB around the world, automated or semiautomated cutting needles have been tested to increase the diagnostic yield [2–8]. We also previously reported on the usefulness of computed tomographic fluoroscopy-guided transthoracic needle biopsy using an 18G automatic biopsy gun for diagnosing pulmonary lesions, particularly benign lesions [9].

The most frequent complication of PNB is pneumothorax, which occurs for 25% to 30% of patients [10]. For fatal complications of PNB, air embolism and tumor seeding have been previously documented to occur. Cases of needle track implantation accounted for almost all of the cases of tumor seeding, and have been documented to occur at a rate of 0% to 3% [11–13]. Although pleural recurrence due to tumor seeding is a possible adverse event that may occur after PNB [14], only two such cases have been reported [15]. Pleural recurrence after PNB tends to be ascribed to the advanced disease itself a priori, but not to PNB, because malignant pleural effusion or tumor dissemination in the pleural cavity can be seen after usual lung surgery without performing a needle biopsy, especially for patients with locally advanced nonsmall cell lung cancer (NSCLC). Thus, in the present study we investigated the risk of pleural recurrence after needle biopsy for patients with pathologic stage I NSCLC, who were thought unlikely to experience recurrence in the pleural cavity after resection.

Material and Methods

Patients

Between October 1986 and December 2000, 687 patients with NSCLC underwent surgical resection of the lung at our hospital. Among them, 335 had pathologic stage I disease, and they constituted the study population. Two hundred patients were men, and the median age was 67 years (range, 35 to 85). The majority of the patients underwent a lobectomy with systematic nodal dissection (n = 256, 76%). Histologic types were adenocarcinoma (n = 222), squamous cell carcinoma (n = 89), and others (n = 24), including large cell carcinoma, large cell neuroendocrine carcinoma, adenosquamous carcinoma, carcinoid, and carcinosarcoma. Primary tumors were classified as T1 in 210 patients and T2 in 125 patients.

Accepted for publication June 27, 2005.

Address correspondence to Dr Matsuguma, Division of Thoracic Surgery, 4-9-13 Yohnan, Utsunomiya, Tochigi 320-0834, Japan; e-mail: hmatsugu@tcc.pref.tochigi.jp.

Published by Elsevier Inc

0003-4975/05/$30.00
doi:10.1016/j.athoracsur.2005.06.074

Treatment Policy

Our routine diagnostic strategies for patients with an indeterminate pulmonary nodule were as follows. First, we obtained a histologic or cytologic diagnosis using fiberoptic bronchoscopy. If this failed or was difficult, the patients were then scheduled for diagnosis using PNB under computed tomography (CT) guidance. Almost all biopsies have been performed using an 18G, spring-loaded, automatic biopsy gun with a modified Tru-Cut type needle (Monopty; Bard Radiology, Convington, Georgia) since 1994 (n = 37), while the Tokyo Medical College needle (n = 12) and the Sure-Cut needle (n = 8) were frequently used before that time. If the state of the nodule remained undetermined, a diagnostic thoracotomy or thoracoscopy was subsequently performed. Some patients underwent intraoperative needle biopsy (INB) whereas the others underwent wedge resection of the lung. If a tumor was diagnosed as NSCLC by intraoperative pathology, the patient subsequently underwent complete resection of the tumor with curative intent. After surgery, the patients were scheduled for checkups, chest radiography, and measurement of serum tumor markers every 1 to 3 months for the first 2 years and every 6 months thereafter. When recurrence was discovered, intrathoracic and extrathoracic lesions were always surveyed.

Assessment of Recurrence and Clinicopathologic Features

We reviewed the medical records of all patients to confirm that recurrence had developed. Pleural recurrence was defined as pleural nodule or malignant effusion or both in the hemithorax of the operated side at the first relapse. Malignant effusion was diagnosed cytologically and pleural dissemination was diagnosed if multiple enhanced pleural nodules were observed on chest CT. Patients with any other site of recurrence in combination with pleural recurrence at the first relapse were included among the pleural recurrence cases, because we can not determine which recurrence preceded and caused the other recurrence. To elucidate the difference of tumor characteristics in each diagnostic group, we reviewed the CT images if available (n = 298) and classified these tumors into two categories according to their locations. When the center of a tumor shadow fell within the inner half of the lung, the tumor was classified as being central; and when the center of a tumor shadow fell within the outer half of the lung, the tumor was classified as being peripheral. We checked whether the tumor shadow was touching the pleura or not on the CT image and then examined the pathologic tumor characteristics such as tumor size, lymphatic invasion, and vascular invasion in the tumor in relation to the diagnostic method used. Pathologic stages were classified according to the criteria set forth by the International System for Staging Lung Cancer [16], and histologic typing was determined according to the World Health Organization classification [17].

Statistical Analysis

Correlations between the diagnostic methods used and the tumor characteristics were examined using the χ^2 test and Fisher's exact test. The unpaired t test was used to examine the relationship between the diagnostic methods used and the log-transformed tumor sizes because of their skewed distribution. All statistical analyses were carried out using STATA software [18].

Results

Among the 335 patients, 290 were diagnosed as having NSCLC preoperatively. Among them, the definitive diagnostic methods used were bronchoscopy for 220, PNB for 66, and sputum cytology for 4. Among the 45 patients with a pulmonary nodule without definitive preoperative diagnosis, INB was performed on 27, wedge resection of the lung on 14, and lung resection with curative intent without definitive diagnosis on 4.

Tumor Characteristics and Diagnostic Methods

The relationships between the methods used to obtain pathologic diagnoses and tumor characteristics are shown in Table 1. Tumors diagnosed by PNB showed less lymphatic invasion and were smaller than those diagnosed by bronchoscopy, and tumors diagnosed by INB were smaller and less invasive than those diagnosed by PNB. When we divided the tumors into two groups according to whether needle biopsy was conducted or not, we found that the needle biopsy group was associated with peripheral location, a smaller tumor size, and a lower occurrence of lymphatic and vascular invasion. Although tumors in the patients of the needle biopsy group were located in more peripheral areas, the numbers of tumors touching the pleura were almost identical. Furthermore, the incidence of pleural invasion of the tumors, which was thought to be associated with pleural recurrence, was lower for the needle biopsy group.

Recurrence

Two hundred and ninety-seven patients (88.7%) were followed up until February 29, 2004. Among the 38 patients not followed-up, 34 completed their follow-up after the 5-year anniversary of surgery. The median length of the follow-up period was 80 months, and the relationships between the methods used for histologic diagnosis and the recurrence patterns are shown in Table 2. Seventy-three patients were diagnosed as having recurrence, where the recurrence pattern was distant for 53 and local for 23. Among them, 3 had distant and local recurrence. Nine patients died of unknown causes; and as 1 patient was diagnosed with distant recurrence at an other hospital, we did not know whether pleural recurrence had developed. For the patients with local recurrence, 10 had pleural recurrence or needle track implantation. The percentage of cases for which distant recurrence had developed was similar between patients diagnosed by bronchoscopy and those diagnosed by PNB (18.5% versus

Table 1. Relationships Between Diagnostic Methods Used and Clinicopathologic Tumor Characteristics

	Diagnostic Methods								
	Preoperative			Intraoperative or Postoperative					
	Bronchoscopic	PNB	Sputum	INB	Wedge	Post	Needle	Nonneedle	*p* Value[a]
Total	220	66	4	27	14	4	93	242	
Clinical									
Sex									
Male	137 (62)	37 (56)	3 (75)	12 (44)	8 (57)	3 (75)	49 (53)	151 (62)	0.105
Female	83 (38)	29 (44)	1 (25)	15 (56)	6 (43)	1 (25)	44 (47)	91 (38)	
Age (years)									
<67	90 (41)	39 (59)	1 (25)	19 (70)	10 (71)	2 (50)	58 (62)	103 (43)	0.001
≥67	130 (59)	27 (41)	3 (75)	8 (30)	4 (29)	2 (50)	35 (38)	139 (57)	
Location									
Peripheral	142 (74)	56 (95)	1 (25)	20 (77)	12 (92)	2 (50)	76 (89)	159 (75)	0.005
Central	50 (26)	3 (5)	3 (75)	6 (23)	1 (8)	2 (50)	9 (11)	54 (25)	
Contact with the pleura									
Yes	91 (47)	32 (54)	2 (50)	8 (30)	6 (46)	1 (25)	40 (47)	100 (47)	0.986
No	101 (53)	27 (46)	2 (50)	18 (70)	7 (54)	3 (75)	45 (53)	113 (53)	
Pathologic									
Histology									
Adenocarcinoma	126 (57)	54 (82)	1 (25)	23 (85)	14 (100)	4 (100)	77 (83)	145 (60)	<0.001
Other	94 (43)	12 (18)	3 (75)	4 (15)	0 (0)	0 (0)	16 (17)	97 (40)	
T factor									
T1	121 (55)	45 (68)	0 (0)	26 (96)	14 (100)	4 (100)	71 (76)	139 (57)	0.001
T2	99 (45)	21 (32)	4 (100)	1 (4)	0 (0)	0 (0)	22 (24)	103 (43)	
Lymphatic invasion									
No	179 (81)	62 (94)	4 (100)	27 (100)	14 (100)	4 (100)	89 (96)	201 (83)	0.002
Yes	41 (19)	4 (6)	0 (0)	0 (0)	0 (0)	0 (0)	4 (4)	41 (17)	
Vascular invasion									
No	138 (63)	49 (74)	1 (25)	26 (96)	14 (100)	3 (75)	75 (81)	156 (64)	0.004
Yes	82 (37)	17 (26)	3 (75)	1 (4)	0 (0)	1 (25)	18 (19)	86 (36)	
Pleural invasion									
No	161 (73)	50 (76)	2 (50)	26 (96)	14 (100)	3 (75)	76 (82)	180 (74)	0.156
Yes	59 (27)	16 (24)	2 (50)	1 (4)	0 (0)	1 (25)	17 (18)	62 (26)	
Tumor size (cm)[b]	2.90	2.38	3.95	1.70	1.20	1.91	2.15	2.75	<0.001

[a] The *p* value for the χ^2 test for the association between needle biopsy and clinicopathologic characteristics in Table 1; [b] Geometric mean.

The numbers in parentheses indicate percentages.

INB = intraoperative needle biopsy; PNB = percutaneous needle biopsy.

15.2%). However, the rate of pleural recurrence for the cases diagnosed by PNB was significantly higher than for the cases diagnosed by bronchoscopy (9.1% versus 1.0%, $p < 0.0028$). The rate of distant recurrence for the cases diagnosed by INB was small at 3.7%, but the proportion with pleural recurrence among the cases diagnosed by INB was as high as that for the cases diagnosed by PNB, at 7.4%. Combining the cases diagnosed by PNB with those diagnosed by INB into the needle biopsy group, the percentage of those affected by pleural recurrence for the needle biopsy group was significantly higher than that for the cases diagnosed using other diagnostic modalities (8.6% versus 0.9%, $p = 0.0009$).

The details of these 10 cases are shown in Table 3. All 10 tumors were adenocarcinoma; and the diagnostic methods used were PNB for 6, INB for 2, and fiberoptic bronchoscopy for 2 patients. Two tumors diagnosed by bronchoscopy showed pleural and vessel invasion that may have been related to pleural recurrence. On the other hand, all 5 pleural recurrence cases showing neither pleural invasion nor vessel invasion in the primary tumor were diagnosed by PNB or INB. The average size of the tumors was 2.7 cm with a range from 1.5 cm to 4.8 cm, and the depth from the visceral pleura to the tumor surface on the needle track during needle biopsy ranged from 0 cm to 2.5 cm. Only 1 patient underwent needle biopsy directly through the

Table 2. Number of Cases According to Recurrence Pattern and Diagnostic Methods Used

	Diagnostic Methods							
	Preoperative			Intraoperative or Postoperative				
	Bronchoscopy	PNB	Sputum	INB	Wedge	Post	Needle	Nonneedle
Number of patients	220[a]	66	4	27	14	4	93	242[a]
Recurrence	48 (22.7)	17 (25.8)	3 (75)	3 (11.1)	2 (14.3)	0 (0)	20 (21.5)	53 (22.7)
Distant	39 (18.5)	10 (15.2)	2 (50)	1 (3.7)	1 (7.1)	0 (0)	11 (11.8)	42 (18.0)
Local	11 (5.2)	8 (12.1)	1 (25)	2 (7.4)	1 (7.1)	0 (0)	10 (10.8)	13 (5.6)
Both distant and local	2	1	0	0	0	0	1	2
Pleural recurrence	2 (1.0)[b]	6 (9.1)	0 (0)	2 (7.4)	0 (0)	0 (0)	8 (8.6)	2 (0.9)[b]
Pleural recurrence alone	2 (1.0)[b]	4 (6.1)	0 (0)	1 (3.7)	0 (0)	0 (0)	5 (5.4)	2 (0.9)[b]

[a] Bronchoscopy group includes 9 uninformative cases for recurrence. Recurrence percentages were calculated excluding the uninformative cases. [b] One patient was uninformative for pleural recurrence.

The numbers in parentheses indicate percentages.

INB = intraoperative needle biopsy; PNB = percutaneous needle biopsy.

pleura attached to the tumor, and for only 2 (cases 1 and 4) the distances were less than 1 cm. In regard to surgical procedures carried out in the 10 patients, lobectomy was performed in 7 patients and segmentectomy in 3 patients (cases 3, 7, and 10). Video-assisted thoracic surgery approach was applied in only 1 INB case; however, subsequent resection was carried out under an open thoracotomy. Concerning the pneumothorax and hemothorax after PNB, 2 cases of pneumothoraces were observed among the 6 patients who underwent PNB. Their relapses occurred 12 to 69 months after surgery, and only 2 patients (cases 4 and 8) with a short follow-up period remained alive with the recurrence.

Comment

A number of needle track implantation cases have been reported, and the incidences were reported at 0% to 3% [12, 13, 19–22]. This rate was considered as negligible by some researchers [12, 23, 24] and as important by the others [15, 25, 26]. On the other hand, pleural recurrence after PNB has not been recognized as a real risk of PNB, although it is theoretically possible adverse event. Only two cases of pleural recurrence after PNB were previously reported [15]. Is the real risk of pleural recurrence due to PNB extremely low? We thought that many cases of pleural recurrence due to PNB may have not been reported because of the difficulty in proving its cause. We

Table 3. Clinicopathologic Characteristics of 9 Cases With Pleural Recurrence and Needle Track Implantation

Case No.	Age (years)/Sex	Diagnostic Methods	Pathologic Findings			Concomitant Recurrence	Time to Recurrence (mo)	Outcome
			Histology	Size (cm)	P/Ly/V			
1	67/M	PNB	P/D Ad	2.2	0/−/−	No	20	DOD
2	68/F	INB	M/D Ad	2.8	0/−/−	Lymphadenopathy	13	DOD
3	72/F	INB	W/D Ad	1.5	0/−/−	No	12	DOD
4	58/F	PNB	M/D Ad	1.9	0/−/−	Pulmonary metastasis	36	AWD
5	50/M	PNB	P/D Ad	4.8	1/−/+	Lymphadenopathy	12	DOD
6	81/F	PNB	M/D Ad	2.5	2/−/−	Lymphangitis	28	DOD
7*	80/F	PNB	W/D Ad	2.6	2/−/−	No	24	DOD
8	76/M	PNB	W/D Ad	1.7	0/−/−	No	69	AWD
9	67/F	Br	P/D Ad	3.2	1/−/+	No	18	DOD
10	74/M	Br	M/D Ad	2.4	1/−/+	No	19	DOD

*Needle track implantation case.

Pleural invasion was judged as being P0 when tumor cells did not invade across the visceral elastic layer, P1 when tumor cells invaded across the visceral elastic layer, and P2 when tumor cells were exposed on the pleural surface.

AWD = alive with disease; Br = bronchoscopy; DOD = dead of disease; F = female; INB = intraoperative needle biopsy; Ly = lymphatic invasion; M = male; M/D Ad = moderately differentiated adenocarcinoma; P = visceral pleural invasion; P/D Ad = poorly differentiated adenocarcinoma; PNB = percutaneous needle biopsy; V = vascular invasion; W/D Ad = well-differentiated adenocarcinoma.

therefore conducted this investigation to elucidate the real risk of pleural recurrence after PNB. We hypothesized that pleural recurrence among patients with resected p-stage I NSCLC, especially with no pleural invasion, lymphatic invasion, and vascular invasion, was less likely to occur after surgery. Pleural recurrence, however, was noted in 9 patients. In addition, 1 case of needle track implantation was found. Among them, 5 cases without pleural and vessel invasion were diagnosed by needle biopsy, and for all an 18G cutting-type needle was used. These results suggested that PNB using this type of needle can cause a plural recurrence in addition to needle track implantation.

Another possible explanation for this high rate of pleural recurrence among the patients in the needle group is the difference in tumor biology between the two groups. Some investigators may believe that tumors diagnosed by PNB are in a peripheral location, and that this may be related to the high rate of pleural recurrence. From our results, we actually found that a peripheral location was more frequently observed for patients in the needle biopsy group. However, the numbers of tumors touching the pleura seen by chest CT were similar for both groups, and pathologic pleural invasion was less frequently observed for those in the needle group. We thought that the smaller size of the tumors for the needle biopsy group contributed to these results, which suggested that the differences in the tumor characteristics did not influence the results. However, we can not exclude the possibility that other tumor characteristics that we did not investigate in this study may have influenced the differences we observed.

The type of the needle we used could influence our high incidence of pleural recurrence. Large-bore cutting needles were replaced by FNA to reduce complications. During the 1990s, since the emergence of the automated and semiautomated cutting needle with an 18G to 20G bore, the cutting needle was used again because of its easy handling and its greater harvest of tissue [3–8]. Some studies compared the accuracy of cutting needle biopsy with FNA and concluded that cutting needle biopsy greatly increases the diagnostic accuracy for cases of benign pulmonary disease [4–6, 8]. On the other hand, for malignant lesions, FNA has the same high diagnostic accuracy as a cutting needle when on-site cytopathology is available [8, 27–29]. In our institute, the automated cutting type biopsy needle was conducted from 1994, and we reported its usefulness for benign lesions [9]. However, in the results from our current study, we encountered one case of needle track implantation among the 66 needle biopsy cases. Although, the incidence of needle track implantation at 1.5% was within the range of the reported incidence, it was on the high side. That the highest incidence of needle track implantation was reported by Harrison and coworkers [21], who used cutting type biopsy needle, suggested that cutting type needle usage could contribute to the tumor seeding. Conversely, more than 10 cases of needle track implantation after FNA have been reported [19, 20, 24, 30–34] since the first reported case by Sinner and Zajicek [13]. Ayar and colleagues [35] conducted a questionnaire study to elucidate the predictive factor for needle track implantation. They collected data on more than 60,000 needle biopsy cases. Among the 8 needle track implantation cases discovered in this study, 5 needle track implantations occurred after the use of 19G to 22G needles, and they concluded that they could not find any predictive factor including needle bore size. The thoroughness of our follow-up could have been related to our high incidence of tumor seeding. Our early stage of this study population has also affected the results. Needle track implantation in patients with early stage lung cancer may be more noticeable when compared with those in patients with more advanced disease because other recurrences may precede and obscure the implanted lesions. The occurrence of pneumothorax or hemithorax after PNB might be associated with the development of pleural recurrence. However, the incidence of hemothorax and pneumothorax among the pleural recurrence cases was 0% and 33 % (2 of 6 patients), and these incidences were not higher than the incidences that we previously reported (0% and 42%) [9].

Only one similar investigation that dealt with the risk of pleural recurrence was reported by Sawabata and colleagues [36]. This group studied 239 patients with completely resected NSCLC of less than 3 cm in maximum diameter and reported that no pleural carcinomatosis occurred for 45 patients who underwent PNB by FNA and wedge resection of the lung. The difference between their study and ours was that their study population included only 22 cases diagnosed by needle biopsy and 71 (30%) with stage II or more advanced disease for which other forms of recurrence could have obscured pleural recurrence.

To avoid the tumor seeding, some researchers have used a coaxial method for which aspiration or the cutting needle passes through an outer needle that stick into the normal lung [5, 6, 28, 37]. However, the effectiveness of this method has not been demonstrated.

The retrospective approach of this study is a weak point. Therefore, we can not conclude from this study that needle biopsy should be avoided. However, the results call doctor's attention to the potential risks faced by needle biopsy and suggest the need for further investigations focusing on pleural recurrence after needle biopsy. To elucidate the real risk of needle biopsy concerning the tumor seeding according to the type of needle or needle size, pleural recurrence and needle track implantation have to be investigated prospectively for patients with early stage lung cancer in multi-institutional setting. Randomized control trial is an ideal method, if possible. When the real risks of pleural recurrence and needle track implantation are discovered, this information will be indispensable for patients who would undergo this needle biopsy.

We thank Satoshi Honjo, MD, of the Epidemiology Unit of the Tochigi Cancer Center for his statistical review, and Yukio Tsuura, MD, of the Pathology Unit of the Tochigi Cancer Center for his pathology review.

References

1. Schreiber G, McCrory DC. Performance characteristics of different modalities for diagnosis of suspected lung cancer: summary of published evidence. Chest 2003;123(Suppl): 115S–28S.
2. Haramati LB. CT-guided automated needle biopsy of the chest. AJR Am J Roentgenol 1995;165:53–5.
3. Wallace MJ, Krishnamurthy S, Broemeling LD, et al. CT-guided percutaneous fine-needle aspiration biopsy of small (< or =1-cm) pulmonary lesions. Radiology 2002;225:823–8.
4. Boiselle PM, Shepard JA, Mark EJ, et al. Routine addition of an automated biopsy device to fine-needle aspiration of the lung: a prospective assessment. AJR Am J Roentgenol 1997; 169:661–6.
5. Klein JS, Salomon G, Stewart EA. Transthoracic needle biopsy with a coaxially placed 20-gauge automated cutting needle: results in 122 patients. Radiology 1996;198:715–20.
6. Moulton JS, Moore PT. Coaxial percutaneous biopsy technique with automated biopsy devices: value in improving accuracy and negative predictive value. Radiology 1993;186: 515–22.
7. Tomiyama N, Mihara N, Maeda M, et al. CT-guided needle biopsy of small pulmonary nodules: value of respiratory gating. Radiology 2000;217:907–10.
8. Greif J, Marmor S, Schwarz Y, Staroselsky AN. Percutaneous core needle biopsy vs. fine needle aspiration in diagnosing benign lung lesions. Acta Cytol 1999;43:756–60.
9. Hirose T, Mori K, Machida S, et al. Computed tomographic fluoroscopy-guided transthoracic needle biopsy for diagnosis of pulmonary nodules. Jpn J Clin Oncol 2000;30:259–62.
10. Tan BB, Flaherty KR, Kazerooni EA, Iannettoni MD. The solitary pulmonary nodule. Chest 2003;123(Suppl):89S–96S.
11. Murphy JM, Gleeson FV, Flower CD. Percutaneous needle biopsy of the lung and its impact on patient management. World J Surg 2001;25:373–9.
12. Lalli AF, McCormack LJ, Zelch M, Reich NE, Belovich D. Aspiration biopsies of chest lesions. Radiology 1978;127:35–40.
13. Sinner WN, Zajicek J. Implantation metastasis after percutaneous transthoracic needle aspiration biopsy. Acta Radiol Diagn (Stockholm) 1976;17:473–80.
14. Sawabata N, Ohta M, Maeda H. Fine-needle aspiration cytologic technique for lung cancer has a high potential of malignant cell spread through the tract. Chest 2000;118: 936–9.
15. Berger RL, Dargan EL, Huang BL. Dissemination of cancer cells by needle biopsy of the lung. J Thorac Cardiovasc Surg 1972;63:430–2.
16. Mountain CF. Revisions in the International System for Staging Lung Cancer. Chest 1997;111:1710–7.
17. World Health Organization. Histological typing of lung and pleural tumours. 3rd ed. Geneva: World Health Organization, 1999.
18. Statacorp. Stata Statistical Software. College Station, TX: Stata Corporation, 2003.
19. Yoshikawa T, Yoshida J, Nishimura M, et al. Lung cancer implantation in the chest wall following percutaneous fine needle aspiration biopsy. Jpn J Clin Oncol 2000;30:450–2.
20. Redwood N, Beggs D, Morgan WE. Dissemination of tumour cells from fine needle biopsy. Thorax 1989;44:826–7.
21. Harrison BD, Thorpe RS, Kitchener PG, McCann BG, Pilling JR. Percutaneous Trucut lung biopsy in the diagnosis of localised pulmonary lesions. Thorax 1984;39:493–9.
22. Nordenstrom B, Bjork VO. Dissemination of cancer cells by needle biopsy of lung. J Thorac Cardiovasc Surg 1973;65:671.
23. Lillington GA. Hazards of transthoracic needle biopsy of the lung. Ann Thorac Surg 1989;48:163–4.
24. Müller NL, Bergin CJ, Miller RR, Ostrow DN. Seeding of malignant cells into the needle track after lung and pleural biopsy. Can Assoc Radiol J 1986;37:192–4.
25. Hix WR, Aaron BL. Needle aspiration in lung cancer. Risk of tumor implantation is not negligible. Chest 1990;97:516–7.
26. Levitt RG. Needle aspiration in lung cancer. Chest 1990;98: 1539–40.
27. Austin JH, Cohen MB. Value of having a cytopathologist present during percutaneous fine-needle aspiration biopsy of lung: report of 55 cancer patients and metaanalysis of the literature. AJR Am J Roentgenol 1993;160:175–7.
28. Lucidarme O, Howarth N, Finet JF, Grenier PA. Intrapulmonary lesions: percutaneous automated biopsy with a detachable, 18-gauge, coaxial cutting needle. Radiology 1998;207: 759–65.
29. McLoud TC. Should cutting needles replace needle aspiration of lung lesions? Radiology 1998;207:569–70.
30. Moloo Z, Finley RJ, Lefcoe MS, Turner-Smith L, Craig ID. Possible spread of bronchogenic carcinoma to the chest wall after a transthoracic fine needle aspiration biopsy. A case report. Acta Cytol 1985;29:167–9.
31. Seyfer AE, Walsh DS, Graeber GM, Nuno IN, Eliasson AH. Chest wall implantation of lung cancer after thin-needle aspiration biopsy. Ann Thorac Surg 1989;48:284–6.
32. Hix WR. Chest wall recurrence of lung cancer after transthoracic fine needle aspiration biopsy. Ann Thorac Surg 1990;50:1020–1.
33. Voravud N, Shin DM, Dekmezian RH, et al. Implantation metastasis of carcinoma after percutaneous fine-needle aspiration biopsy. Chest 1992;102:313–5.
34. Raftopoulos Y, Furey WW, Kacey DJ, Podbielski FJ. Tumor implantation after computed tomography-guided biopsy of lung cancer. J Thorac Cardiovasc Surg 2000;119:1288–9.
35. Ayar D, Golla B, Lee JY, Nath H. Needle-track metastasis after transthoracic needle biopsy. J Thorac Imaging 1998;13: 2–6.
36. Sawabata N, Maeda H, Ohta M, Hayakawa M. Operable non-small cell lung cancer diagnosed by transpleural techniques: do they affect relapse and prognosis? Chest 2001;120: 1595–8.
37. Hayashi N, Sakai T, Kitagawa M, et al. CT-guided biopsy of pulmonary nodules less than 3 cm: usefulness of the spring-operated core biopsy needle and frozen-section pathologic diagnosis. AJR Am J Roentgenol 1998;170:329–31.

TECHNICAL NOTE

Radiation Medicine: Vol. 23 No. 3, 216–219 p.p., 2005

Simple Technique to Visualize Random Set-up Displacements Using a Commercially Available Radiotherapy Planning System

Hiromichi Ishiyama,* Masashi Kitano,* Yuzuru Niibe,* Mineko Uemae, and Kazushige Hayakawa***

Purpose: To visualize random set-up displacements in isodose distribution images, we introduce a simple technique using a commercially available radiotherapy planning system (RTP).
Materials and Methods: A distribution of set-up displacement is known to be compatible with that of a Gaussian distribution. Based on that assumption, 41 intentionally misaligned beams with 1-mm intervals were planned in the respective weights according to Gaussian distribution. "Modified" isodose distributions were then visualized using a commercially available RTP. In the next step, only two beams misaligned with one standard deviation (SD) of the Gaussian distribution were used in place of 41 beams, as a large number of beams increases the workload and is unsuitable for clinical use. Differences between the two versions of isodose distribution images were assessed visually.
Results: In modified dose distribution images, the edge of distribution was dull compared to normal images. These images show that the larger SD of set-up displacement dulls the edge of dose distribution. Images from two beams were not significantly different to those from 41 beams.
Conclusion: Using this technique, the impact of random set-up displacements was effectively reflected in isodose distribution images.

Key words: set-up displacement, radiotherapy, treatment simulation

Introduction

Geometrical uncertainties in radiotherapy cause differences between intended and actual delivered dose distributions. One of the major causes of uncertainties is set-up displacement.

Set-up displacement can involve systematic and/or random displacement.[1] Systematic displacement comprises the same displacement for each fraction of treatment, whereas random displacement varies from day to day. By measuring set-up displacement several times, the typical sizes of systematic and random displacement can be determined,[2] and the standard deviation (SD) of set-up displacement is reportedly 1.0-5.0 mm for currently applied treatment techniques.[3] In addition, distributions of set-up displacements for all three directions are compatible with that of a Gaussian distribution because of a large number of set-up procedures,[4] and the average and SD of Gaussian distributions are compatible with systematic and random set-up displacement, respectively.

Usually, the margin to expand clinical target volume (CTV) to obtain sufficient tumor coverage is planned empirically by physicians. However, empirical methods could represent a cause of decreased tumor control and increased complications involving normal tissues. In particular, with the recent advent of computed tomography (CT) simulations, isodose distribution images are crucial because of heavy dependence on them by physicians and physicists. For more precise and reasonable planning, we believe that visualization of set-up displacement in isodose distribution images is needed.

This report introduces and assesses a simple technique for visualizing random set-up displacements using a commercially available radiotherapy planning system (RTP).

Received July 16, 2004; revision accepted October 8, 2004.

*Department of Radiology, Kitasato University School of Medicine

**Division of Radiation Oncology, Kitasato University Hospital

Reprint requests to Hiromichi Ishiyama, M.D., Department of Radiology, Kitasato University Hospital, 1-15-1 Kitasato, Sagamihara, Kanagawa 228-8555, JAPAN.

Materials and Methods

Phantom study

A solid water phantom (Solid Water®, Gammex RMI, Middleton, WI, USA) was scanned with a CT simulator using a slice thickness and interval of 5 mm. All images were transferred to a three-dimensional treatment planning system (Pinnacle³®, version 6.5b, ADAC Co., USA). Anterior 10 cm×10 cm irradiations with 4 MV photons were planned. Isodose curves of 110%, 107%, 100%, 95%, 90%, 80%, 70%, 60%, 50%, 40%, 30%, 20%, and 10% relative to an isocenter dose were displayed as a "normal" isodose distribution.

On the assumption that translations of set-up displacements would occur between −20 mm and +20 mm, 41 intentionally misaligned beams were planned with 1-mm intervals along the horizontal axis. Considering the isodose distribution of a total treatment course all at once, the number of fractions at each misaligned beam could be considered the weight of those respective beams. To calculate the weight of each misaligned beam, values of density function of the Gaussian distribution were used. The operational window of Excel software (Microsoft, USA) was used for value calculations (Fig. 1). The average of Gaussian distributions was set on 0 mm, and SDs were set on 1-5 mm, with 1-mm intervals. The five Gaussian distributions were therefore calculated for different SDs and were visualized as "modified" isodose distributions.

Modified isodose distribution images were visually compared with normal isodose distribution images.

Simplification for clinical use

Although a greater number of intentionally misaligned beams makes the Gaussian distribution smoother and more accurate, the workload of operators would be significantly increased. We therefore needed to decrease the number of misaligned beams for clinical use. In principle, as few as two symmetric beams misaligned within 1 SD can be used as a substitute for the large number of misaligned beams, because SD is statistically defined in the literature as a "standard" of deviations. Modified isodose distribution images from two beams were visually compared with those from 41 beams.

Results

"Normal" and "modified" isodose distributions were calculated from 41 beams or two beams (Fig. 2). In modified images, the edge of the distribution was dull

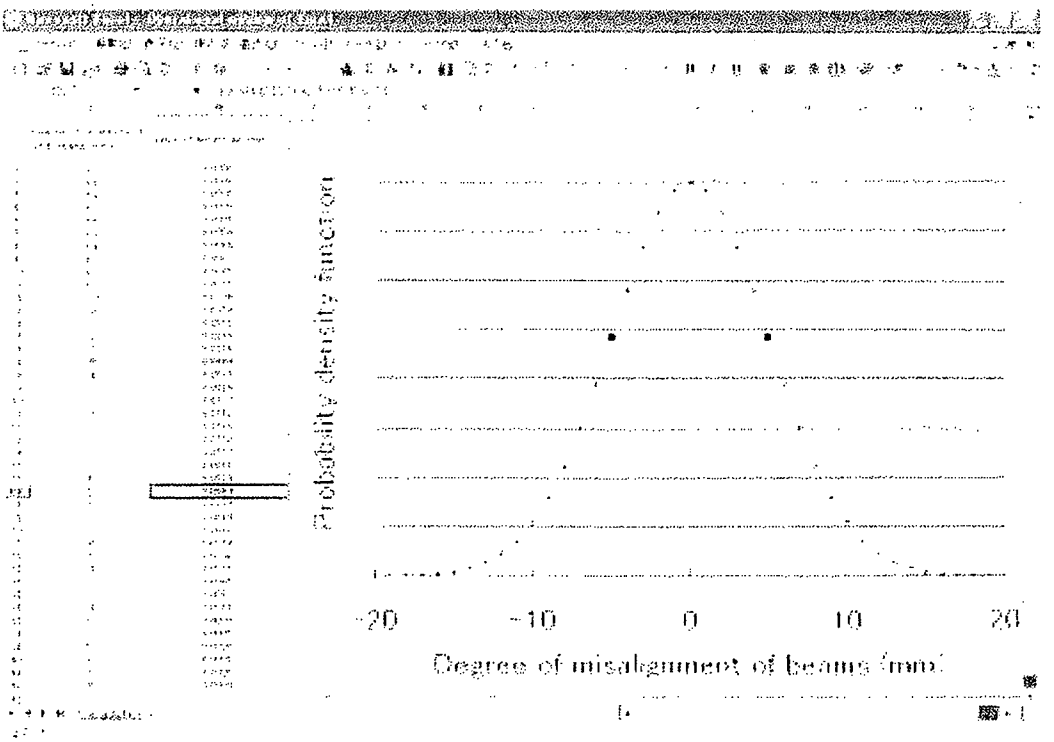

Fig. 1. Values of density function of the Gaussian distribution were calculated using the "NORMDIST" function of Excel software (Microsoft). For calculating the modified isodose distributions from two beams, a pair of symmetric beams misaligned with 1 SD was used (large points in the distribution).